JOURNAL OF COMPUTATIONAL PHYSICS 68, 327–345 (1987)

Calculation of Extinction Limits for Premixed Laminar Flames in a Stagnation Point Flow*

V. GIOVANGIGLI

Laboratoire de Mécanique Théorique, Université Paris, and Laboratoire d'Énergétique, École Centrale des Arts et Manufactures, France

AND

M. D. SMOOKE

Department of Mechanical Engineering, Yale University, New Haven, Connecticut

Received September 13, 1985; revised February 18, 1986

Conclusions derived from the solution of premixed laminar flames in a stagnation point flow are important in the study of pollutant formation, the determination of chemically controlled extinction limits and in the ability to characterize the combustion processes occurring in turbulent flames. In the neighborhood of the stagnation point produced in these flames, a chemically reacting boundary layer is established. For a given equivalence ratio, the input flow velocity can be varied and solutions can be determined for increasing values of the strain rate. As the strain rate increases, the flame nears extinction. In the vicinity of the extinction point, however, the Jacobian of the system becomes singular. To avoid computational difficulties, we employ numerical bifurcation techniques to generate the approriate steady-state profiles (both physical and nonphysical). The method is applied to study the extinction behavior of a one-step kinetics model of a premixed hydrogen–air and methane–air flame in a counterflow geometry.

1. INTRODUCTION

Conclusions derived from the solution of premixed laminar flames in a stagnation point flow are important in the determination of chemically controlled extinction limits, in the ability to characterize the combustion processes occurring in turbulent flames and in the study of pollutant formation. Experimentally these flames can be produced by a single reactant stream impinging on an adiabatic wall or by two counterflowing reactant streams emerging from two coaxial jets. In the neighborhood of the stagnation point produced by these flows, a chemically reacting boundary layer is established. Along the stagnation point streamline the

* Work supported by the Office of Naval Research.

0021-9991/87 $3.00

governing equations can be reduced to a system of coupled nonlinear two-point boundary value problems. In the single reactant stream configuration only one reaction zone is produced. If the exit velocity and the equivalence ratio of the fuel–air mixture of each jet are equal, then in the two reactant stream problem a double flame is produced with a plane of symmetry through the stagnation point and parallel to the two jets (see Fig. 1).

A number of studies of premixed flames in a stagnation point flow have appeared recently in the literature [1–13]. The work has focused on experimental [1–3, 8, 13], analytical [4, 5, 9, 12], and numerical investigations [6, 7, 10–12]. In several of these studies a single reactant jet was utilized [1, 2, 4–7, 10, 12, 13] while in others two counterflowing reactant streams were employed [1, 3, 8, 9, 11]. In a number of cases it was found that the Lewis number played an important role in the behavior of these flames near extinction. Computationally, for a given equivalence ratio, the input flow velocity can be varied and one can obtain a relationship between the strain rate (the velocity gradient) and the peak temperature. In general, as the input flow velocity is increased and the flame nears extinction, the peak temperature decreases. It is in the neighborhood of the extinction point, however, that computation of the solution often becomes difficult. In particular, at the extinction point one can show that the Jacobian of the system is singular. If solutions are desired in this region, the computational procedure must be modified to account for the singular behavior of the system.

Procedures enabling the calculation of bifurcation and limit points for systems of nonlinear equations have been discussed, for example, by Keller [14], Jepson and Spence [15], Chan [16], Seydel [17], and Heinemann, Overholser, and Reddien [18, 19]. In particular, in the work of Heinemann *et al.* a version of Keller's arc-length continuation method was used to calculate the multiple steady states of a model one-step, nonadiabatic, premixed laminar flame [18] and a premixed, nonadiabatic, hydrogen–air system [19]. In the hydrogen–air problem the cold boundary temperature was taken as the bifurcation parameter and *S*-shaped response curves with both an ignition and an extinction point were obtained.

In this paper we focus our attention on doubly premixed laminar flames produced by two counterflowing coaxial jets. By applying appropriate boundary

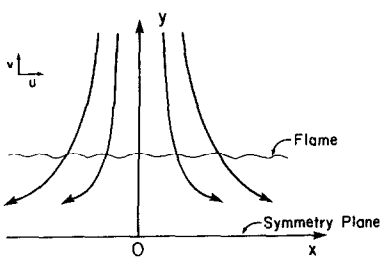

FIG. 1. Schematic of the stagnation point flow configuration.

conditions at the plane of symmetry, the model we consider is, in principle, equivalent to that of a single reactant stream impinging on an adiabatic wall with slip. Our goal is to generalize the ideas used in [18, 19] so that extinction limits of premixed laminar flames in a stagnation point flow can be calculated. In particular, we solve the governing conservation equations of mass, momentum, species, and energy by an adaptive finite difference procedure. In our model the strain rate (or more precisely the inverse of the strain rate) is the natural bifurcation parameter. However, as the strain rate is increased and the flame nears extinction, the Jacobian of our system becomes singular. We overcome this difficulty by applying a modification of the arc-length continuation procedure used in [18, 19]. Specifically, by introducing the bifurcation parameter as an eigenvalue at each grid point and by modifying the pseudo-arclength boundary condition, we can maintain the block tridiagonal structure of the Jacobian matrix. In this way we do not have to modify our linear equation solver as would be the case if the approach used in [18, 19] were employed. To simplify the computations, we assume all the Lewis numbers are equal to one and we employ a global one-step kinetics model. We investigate the extinction properties of both premixed hydrogen–air and methane–air flames. We observe C-shaped extinction curves similar to the ones obtained by Smith *et al.* [10] and Giovangigli and Candel [12]. We realize, of course, that a one-step procedure cannot predict adequately the effects of nonunit Lewis numbers of the deficient reactants on extinction. Nevertheless, the approach we take illustrates the effectiveness of the numerical bifurcation procedure in calculating the multiple steady states of these particular flames. Ultimately, we will apply the methods used in this paper to study the effects of finite rate kinetics on the extinction of premixed hydrogen–air and methane–air flames in a counterflow geometry.

The organization of the paper is such that in the next section we present the governing conservation equations and in Section 3 we formulate the one-step model. In Section 4 we outline the boundary value solution method and in Section 5 we discuss the modified arclength continuation procedure. Numerical results are presented in Section 6.

2. Problem Formulation

Our model for counterflowing premixed flames assumes the flow to be laminar, stagnation point flow. Hence, the governing boundary layer equations for mass, momentum, chemical species, and energy can be written in the form

$$\frac{\partial(\rho u x^{\alpha})}{\partial x} + \frac{\partial(\rho v x^{\alpha})}{\partial y} = 0, \tag{2.1}$$

$$\rho u \frac{\partial u}{\partial x} + \rho v \frac{\partial u}{\partial y} + \frac{\partial p}{\partial x} = \frac{\partial}{\partial y}\left(\mu \frac{\partial u}{\partial y}\right), \tag{2.2}$$

$$\rho u \frac{\partial Y_k}{\partial x} + \rho v \frac{\partial Y_k}{\partial y} + \frac{\partial}{\partial y}(\rho Y_k V_{ky}) - \dot{w}_k W_k = 0, \qquad k = 1, 2, \ldots, K, \tag{2.3}$$

$$\rho u c_p \frac{\partial T}{\partial x} + \rho v c_p \frac{\partial T}{\partial y} - \frac{\partial}{\partial y}\left(\lambda \frac{\partial T}{\partial y}\right) + \sum_{k=1}^{K} \rho Y_k V_{ky} c_{pk} \frac{\partial T}{\partial y} + \sum_{k=1}^{K} \dot{w}_k W_k h_k = 0, \tag{2.4}$$

where α represents a geometric factor ($\alpha = 0$ for cartesian coordinates and $\alpha = 1$ for cylindrical coordinates). For the remainder of this paper we set $\alpha = 0$. The system is closed with the ideal gas law,

$$\rho = p\bar{W}/RT. \tag{2.5}$$

In these equations x and y denote independent spatial coordinates; T, the temperature; Y_k, the mass fraction of the kth species; p, the pressure; u and v the tangential and the transverse components of the velocity, respectively; ρ, the mass density; W_k, the molecular weight of the kth species; $\bar{W}$, the mean molecular weight of the mixture; R, the universal gas constant; λ, the thermal conductivity of the mixture; c_p, the constant pressure heat capacity of the mixture; c_{pk}, the constant pressure heat capacity of the kth species; $\dot{w}_k$, the molar rate of production of the kth species per unit volume; h_k, the specific enthalpy of the kth species; μ the viscosity of the mixture and V_{ky} is the diffusion velocity of the kth species in the y direction. The free stream (tangential) velocity at the edge of the boundary layer is given by $u_e = ax$ where a is the strain rate.

We introduce the notation

$$f' = u/u_e, \tag{2.6}$$

$$V = \rho v, \tag{2.7}$$

where f' is related to the derivative of a modified stream function (see, e.g., Dixon-Lewis *et al.* [20]). Using these expressions, the boundary layer equations can be transformed into a system of ordinary differential equations valid along the stagnation-point streamline $x = 0$. For a system in rectangular coordinates, we have

$$\frac{dV}{dy} + a\rho f' = 0, \tag{2.8}$$

$$\frac{d}{dy}\left(\mu \frac{df'}{dy}\right) - V \frac{df'}{dy} + a(\rho_e - \rho(f')^2) = 0, \tag{2.9}$$

$$-\frac{d}{dy}(\rho Y_k V_k) - V \frac{dY_k}{dy} + \dot{w}_k W_k = 0, \qquad k = 1, 2, \ldots, K, \tag{2.10}$$

$$\frac{d}{dy}\left(\lambda \frac{dT}{dy}\right) - c_p V \frac{dT}{dy} - \sum_{k=1}^{K} \rho Y_k V_k c_{pk} \frac{dT}{dy} - \sum_{k=1}^{K} \dot{w}_k W_k h_k = 0. \tag{2.11}$$

At the plane of symmetry ($y = 0$) the boundary conditions are given by

$$V = 0, \tag{2.12}$$

$$df'/dy = 0, \tag{2.13}$$

$$dY_k/dy = 0, \qquad k = 1, 2,..., K, \tag{2.14}$$

$$dT/dy = 0, \tag{2.15}$$

and as $y \to \infty$ by

$$f' = 1, \tag{2.16}$$

$$Y_k = Y_{k_e}, \qquad k = 1, 2,..., K, \tag{2.17}$$

$$T = T_e. \tag{2.18}$$

The mass fractions Y_{k_e}, $k = 1, 2,..., K$ and the temperature T_e at the edge of the boundary layer are specified quantities.

3. One-Step Model

Most complex combustion systems ordinarily involve large numbers of chemical species. These species are related through a detailed kinetics mechanism involving many elementary chemical reactions. Solution of the governing equations in such systems reduces to the solution of an ordinary or partial differential equation for each species mass fraction. In some applications the determination of the appropriate chemical reactions and their respective rate constants can be a difficult task. It can be made simpler, however, by postulating a single global reaction for the system. This can also be useful when the size of the system to be solved (for the computer being used) results in a computationally infeasible problem. We realize, of course, that a global reaction mechanism does not provide detailed information on the system's minor species–information that is often needed in assessing the detailed structure of a reacting system (see, e.g., [21, 22]).

Determination of overall, global, reaction rates for flames has been investigated, for example, by Levy and Weinberg [23, 24], Westbrook and Dryer [25] and Coffee, Kotlar, and Miller [26]. In the paper by Coffee *et al.*, the equations governing freely propagating, premixed, laminar flames with detailed kinetics and complex transport were solved for the temperature and the species mass fractions. From the calculated temperature, a heat release profile was obtained as a function of the independent spatial coordinate. The reaction rate parameters could then be obtained by a two-parameter least squares fit to this data. In this paper we utilize these calculated reaction rate parameters in the numerical solution of one-step, premixed, laminar hydrogen–air and methane–air flames in a counterflow geometry.

We assume the fuel and the oxidizer obey a single overall irreversible reaction of the type

$$\text{Fuel } (F) + \text{Oxidizer } (O) \to \text{Products } (P), \tag{3.1}$$

in the presence of an inert gas (N). We have

$$\nu_F F + \nu_O O \rightarrow \nu_P P, \tag{3.2}$$

where ν_F, ν_O, and ν_P are the stoichiometric coefficients of the fuel, the oxidizer and the product, respectively. In addition, in the one-step model we consider, we neglect thermal diffusion and we assume that the ordinary mass diffusion velocities can be written in terms of Fick's law, i.e.,

$$V_k = -\frac{D_k}{Y_k}\frac{dY_k}{dy}, \qquad k = 1, 2, \ldots, K, \tag{3.3}$$

where D_k is the diffusion coefficient of the kth species into the mixture. We also take the quantities $c_p = c_{pk}$, $\rho\lambda$, $\rho^2 D_k$, and $\rho\mu$ to be constant.

If, for purposes of the discussion that follows, we introduce the Lewis number of each species

$$\mathrm{Le}_F = \frac{\lambda}{\rho D_F c_p}, \qquad \mathrm{Le}_O = \frac{\lambda}{\rho D_O c_p}, \tag{3.4a}$$

$$\mathrm{Le}_P = \frac{\lambda}{\rho D_P c_p}, \qquad \mathrm{Le}_N = \frac{\lambda}{\rho D_N c_p}, \tag{3.4b}$$

and the Prandtl number

$$\mathrm{Pr} = \mu c_p/\lambda, \tag{3.5}$$

then the governing equations in (2.8–2.11) become

$$\frac{dV}{dy} + a\rho f' = 0, \tag{3.6}$$

$$\mathrm{Pr}\frac{d}{dy}\left(\frac{\lambda}{c_p}\frac{df'}{dy}\right) - V\frac{df'}{dy} + a(\rho_e - \rho(f')^2) = 0, \tag{3.7}$$

$$\frac{1}{\mathrm{Le}_F}\frac{d}{dy}\left(\frac{\lambda}{c_p}\frac{dY_F}{dy}\right) - V\frac{dY_F}{dy} - W_F\nu_F\dot{w} = 0, \tag{3.8}$$

$$\frac{1}{\mathrm{Le}_O}\frac{d}{dy}\left(\frac{\lambda}{c_p}\frac{dY_O}{dy}\right) - V\frac{dY_O}{dy} - W_O\nu_O\dot{w} = 0, \tag{3.9}$$

$$\frac{1}{\mathrm{Le}_P}\frac{d}{dy}\left(\frac{\lambda}{c_p}\frac{dY_P}{dy}\right) - V\frac{dY_P}{dy} + W_P\nu_P\dot{w} = 0, \tag{3.10}$$

$$\frac{1}{\mathrm{Le}_N}\frac{d}{dy}\left(\frac{\lambda}{c_p}\frac{dY_N}{dy}\right) - V\frac{dY_N}{dy} = 0, \tag{3.11}$$

$$\frac{d}{dy}\left(\frac{\lambda}{c_p}\frac{dT}{dy}\right) - V\frac{dT}{dy} + \frac{(W_F\nu_F h_F + W_O\nu_O h_O - W_P\nu_P h_P)}{c_p}\dot{w} = 0, \tag{3.12}$$

where

$$\dot{w} = -\frac{\dot{w}_F}{\nu_F} = -\frac{\dot{w}_O}{\nu_O} = \frac{\dot{w}_P}{\nu_P}, \tag{3.13}$$

is the rate of progress of the reaction and where we have made use of the fact that $\sum_{k=1}^{K} Y_k V_k = 0$. From Eq. (3.11) we see that the inert gas profile $Y_N = Y_{N_e} =$ constant.

If we now assume that the Lewis numbers and the Prandtl number are equal to one and if we introduce the heat release per unit mass of the fuel Q, where

$$Q = h_F + \frac{W_O \nu_O}{W_F \nu_F} h_O - \frac{W_P \nu_P}{W_F \nu_F} h_P, \tag{3.14}$$

we can derive the following Shvab–Zeldovich relations

$$Y_F = Y_{F_e} - \frac{c_p}{Q}(T - T_e), \tag{3.15}$$

$$Y_O = Y_{O_e} - \frac{c_p}{Q}\frac{W_O \nu_O}{W_F \nu_F}(T - T_e), \tag{3.16}$$

$$Y_P = Y_{P_e} + \frac{c_p}{Q}\frac{W_P \nu_P}{W_F \nu_F}(T - T_e). \tag{3.17}$$

With the rate of progress given by an Arrhenius type relation, the heat release per unit volume can be written in the form

$$q = Q W_F \nu_F \dot{w} = Q(\rho Y_F)^{\nu_F}(\rho Y_O)^{\nu_O} A \exp(-E/RT), \tag{3.18}$$

and the one-step model reduces to the solution of

$$\frac{dV}{dy} + a\rho f' = 0, \tag{3.19}$$

$$\frac{d}{dy}\left(\frac{\lambda}{c_p}\frac{df'}{dy}\right) - V\frac{df'}{dy} + a(\rho_e - \rho(f')^2) = 0, \tag{3.20}$$

$$\frac{d}{dy}\left(\frac{\lambda}{c_p}\frac{dT}{dy}\right) - V\frac{dT}{dy} + \frac{q}{c_p} = 0, \tag{3.21}$$

with the boundary conditions at $y = 0$ given by

$$V = 0, \tag{3.22}$$

$$\frac{df'}{dy} = 0, \tag{3.23}$$

$$\frac{dT}{dy} = 0, \tag{3.24}$$

and as $y \to \infty$ by

$$f' = 1, \tag{3.25}$$

$$T = T_e. \tag{3.26}$$

We observe that, as a result of (3.15)–(3.18) and the ideal gas law, the expression for q in (3.21) is strictly a function of the temperature and, in addition to the stoichiometry of the global reaction, it depends upon the heat release per unit mass of the fuel, the edge temperature and mass fractions, and the two Arrhenius parameters. We also point out that, as the strain rate approaches zero, the flame will shift further and further from the plane of symmetry so that (up to an arbitrary translation) it eventually approaches a freely propagating premixed laminar flame. As a result, in the calculations reported in Section 6, we use the values of the heat release Q and the two Arrhenius constants A and E that were obtained by Coffee *et al.* [26] from a set of detailed chemistry calculations of freely propagating premixed laminar flames. In their investigation the adiabatic flame temperature of a detailed chemistry model was used to determine the value of the heat release per unit mass. The parameters A and E were then determined by a least squares fit such that

$$A \exp(-E/RT^*) \approx q^*/Q(\rho(T^*)\, Y_F(T^*))^{\nu_F}(\rho(T^*)\, Y_O(T^*))^{\nu_O}, \tag{3.27}$$

where (T^*, q^*) are the temperatures and heat releases from the detailed chemistry model.

4. Method of Solution

Solution of Eqs. (3.19)–(3.26) proceeds by an adaptive nonlinear boundary value method. The solution procedure has been discussed in detail elsewhere [27] and we outline only the essential features here. Our goal is to obtain a discrete solution of the governing equations on the mesh $\mathcal{M}$

$$\mathcal{M} = \{0 = y_0 < y_1 < \cdots < y_m = L\}, \tag{4.1}$$

where $h_j = y_j - y_{j-1}$, $j = 1, 2, \ldots, m$, and where the value of L is taken large enough so that the zero flux boundary conditions are satisfied to an acceptable level of accuracy. We approximate spatial derivatives with finite difference expressions. Specifically, we write

$$\frac{d}{dy}\left(a(y)\frac{dg}{dy}\right)_{y_j} \approx \left(\frac{2}{y_{j+1} - y_{j-1}}\right)(a_{j+1/2}\partial g_{j+1} - a_{j-1/2}\partial g_j), \tag{4.2}$$

where we define $g_j = g(y_j), j = 0, 1, \ldots, m$, and

$$g_{j+1/2} = \frac{(g_{j+1} + g_j)}{2}, \qquad j = 0, 1, \ldots, m-1, \tag{4.3}$$

$$\partial g_{j+1} = \frac{(g_{j+1} - g_j)}{h_{j+1}}, \qquad j = 0, 1, \ldots, m-1. \tag{4.4}$$

First derivatives are differenced using upwind difference expressions.

Newton's Method

With the continuous differential operators replaced by expressions similar to those in (4.2)–(4.4), we convert the problem of finding an analytic solution of the governing equations to one of finding an approximation to this solution at each point of the mesh $\mathcal{M}$. We seek the solution U_h^* of the nonlinear system of difference equations

$$F(U_h^*) = 0. \tag{4.5}$$

For an initial solution estimate U^0 that is sufficiently "close" to U_h^*, the system of equations in (4.5) can be solved by Newton's method. We write

$$J(U^k)(U^{k+1} - U^k) = -\lambda_k F(U^k), \qquad k = 0, 1, \ldots, \tag{4.6}$$

where U^k denotes the kth solution iterate, λ_k the kth damping parameter ($0 < \lambda \leqslant 1$) [28] and $J(U^k) = \partial F(U^k)/\partial U$ the Jacobian matrix. A system of linear block tridiagonal equations must be solved at each iteration for corrections to the previous solution vector. For many problems the cost of forming (either analytically or numerically) and factoring the Jacobian matrix can be a significant part of the cost of the total calculation. In such problems we apply a modified Newton method in which the Jacobian is re-evaluated only periodically [29].

Adaptive Gridding

Solution of boundary value problems by finite difference methods requires that a mesh be determined a priori. Many of the methods that have been used to determine adaptive grids for two-point boundary value problems can be interpreted in terms of equidistributing a positive weight function over a given interval [30, 31]. We say that a mesh $\mathcal{M}$ is equidistributed on the interval $[0, L]$ with respect to the non-negative function W and the constant C if

$$\int_{y_j}^{y_{j+1}} W \, dy = C, \qquad j = 0, 1, \ldots, m-1. \tag{4.7}$$

The major differences in the various approaches center around the choice of the weight function and whether or not the mesh is coupled with the calculation of the dependent solution components (see, e.g., [32, 33]). We determine the mesh (see

[27]) by employing a weight function that equidistributes the difference in the components of the discrete solution and its gradient between adjacent mesh points. Upon denoting the vector of N dependent solution components by $\tilde{U} = [\tilde{U}_1, \tilde{U}_2, ..., \tilde{U}_N]^T$, we seek a mesh $\mathcal{M}$ such that

$$\int_{y_j}^{y_{j+1}} \left| \frac{d\tilde{U}_i}{dy} \right| dy \leqslant \delta \left| \max_{0 \leqslant y \leqslant L} \tilde{U}_i - \min_{0 \leqslant y \leqslant L} \tilde{U}_i \right| \quad j = 0, 1, ..., m-1, \; i = 1, 2, ..., N, \tag{4.8}$$

and

$$\int_{y_j}^{y_{j+1}} \left| \frac{d^2\tilde{U}_i}{dy^2} \right| dy \leqslant \gamma \left| \max_{0 \leqslant y \leqslant L} \frac{d\tilde{U}_i}{dy} - \min_{0 \leqslant y \leqslant L} \frac{d\tilde{U}_i}{dy} \right| \quad j = 1, 2, ..., m-1, \; i = 1, 2, ..., N, \tag{4.9}$$

where δ and γ are small numbers less than one and the maximum and minimum values of $\tilde{U}_i$ and $d\tilde{U}_i/dy$ are obtained from a converged numerical solution on a previously determined mesh.

A potential problem of such an equidistribution procedure is the formation of a mesh that may not be smoothly varying. For example, the ratio of consecutive mesh intervals may differ by several orders of magnitude. This can affect the accuracy of the method as well as the convergence properties of the Newton iteration. As a result, we impose the added constraint that the mesh produced by employing (4.8) and (4.9) be locally bounded, i.e., the ratio of adjacent mesh intervals must be bounded above and below by constants. We require

$$\frac{1}{A} \leqslant \frac{h_j}{h_{j-1}} \leqslant A, \qquad j = 2, 3, ..., m, \tag{4.10}$$

where A is a constant $\geqslant 1$. This smooths out rapid changes in the size of the mesh intervals.

In employing the adaptive mesh algorithm, we first solve the boundary value problem on a coarse mesh and obtain the maximum and minimum values of $\tilde{U}_i$ and $d\tilde{U}_i/dy$. The inequalities in (4.8)–(4.10) are then tested and if any of them is not satisfied, a grid point is inserted at the midpoint of the interval in question. Once a new mesh has been obtained, the previously converged numerical solution is interpolated onto the new mesh. The problem is solved on the new mesh and the process continues until (4.8)–(4.10) are satisfied.

5. Arclength Continuation

We observe that the system of equations in (4.5) can be written in the form

$$F(U, 1/a) = 0, \tag{5.1}$$

where specific reference to the parametric dependence on the inverse of the strain

rate has been made. (The inverse of the strain rate is used, as opposed to the strain rate itself, due to its relationship to the Damköhler number [9]). As the value of a increases and the flame nears extinction, the maximum value of the temperature decreases. It is near the extinction limit, however, that the numerical calculations become increasingly difficult. In particular, at the extinction point the Jacobian of the system is singular. To alleviate the computational difficulties, a modified form of the governing equations is solved [14]. We introduce the reciprocal of the strain rate as a new dependent variable. The vector of dependent variables $(U, 1/a)^T$ can now be considered functions of a new independent parameter s. If we define

$$Z(s) = (U(s), 1/a(s))^T, \tag{5.2}$$

then the new problem we want to solve is given by

$$G(Z, s) = 0, \tag{5.3}$$

where

$$G(Z, s) = \begin{bmatrix} F(U(s), 1/a(s)) \\ N(U(s), 1/a(s), s) \end{bmatrix} = \begin{bmatrix} F(Z(s)) \\ N(Z(s), s) \end{bmatrix}, \tag{5.4}$$

and where N is an arbitrary normalization. As is often the case, (see, e.g., [14]) the normalization is chosen such that s approximates the arclength of the solution branch in the space $(\|U\|, 1/a)$ (see Fig. 2). As an example, if $(U(s_0), 1/a(s_0))^T$ is a known solution, then two commonly used normalizations are

$$N_1 = \theta \left(\frac{dU(s_0)}{ds} \right)^T (U(s) - U(s_0)) + (1-\theta) \frac{d}{ds} \left(\frac{1}{a(s_0)} \right) \left(\frac{1}{a(s)} - \frac{1}{a(s_0)} \right) - (s - s_0) = 0, \tag{5.5}$$

and

$$N_2 = \theta \|U(s) - U(s_0)\|^2 + (1-\theta) \left(\frac{1}{a(s)} - \frac{1}{a(s_0)} \right)^2 - (s - s_0)^2 = 0, \tag{5.6}$$

where $\theta \in (0, 1)$.

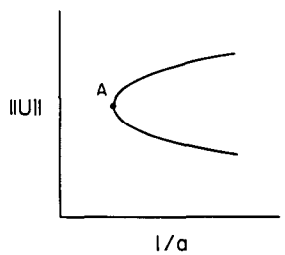

FIG. 2. Bifurcation diagram illustrating a simple turning point (A).

The Jacobian of the new system can be written in the form

$$\mathcal{J}(Z, s) = G_Z(Z, s) = \begin{bmatrix} F_U(U(s), 1/a(s)) & F_{1/a}(U(s), 1/a(s)) \\ N_U(U(s), 1/a(s), s) & N_{1/a}(U(s), 1/a(s), s) \end{bmatrix}, \tag{5.7}$$

where F_U, $F_{1/a}$, N_U, and $N_{1/a}$ denote the appropriate partial derivatives. It can be shown that at a simple turning point, even though F_U is singular $\mathcal{J}$ is not. In addition, given a solution $Z(s)$ we can determine a new predicted value for $Z(s+\delta s)$ by forming

$$Z(s+\delta s) = Z(s) + \frac{dZ}{ds}\delta s, \tag{5.8}$$

where dZ/ds is determined from

$$\mathcal{J}\frac{dZ}{ds} = \begin{bmatrix} 0 \\ N_s(Z(s), s) \end{bmatrix}. \tag{5.9}$$

Several points are worth discussing in more detail. As a result of the differencing used in (4.2)–(4.4), the Jacobian of the system in (4.5) is block tridiagonal. However, if after introduction of the reciprocal of the strain rate as a dependent variable along with the extra normalization condition, the quantities $F_{1/a}$ and N_U are not of the proper form, the block tridiagonal structure of the Jacobian will be destroyed. For the normalizations considered in (5.5) and (5.6) this is ordinarily the case. Although solution of the system of linear equations corresponding to (5.3) can proceed by methods discussed in [16], we would like to keep the basic block tridiagonal structure of the Jacobian. In this way we can utilize the solution method used in solving adiabatic, premixed, laminar flames [34], burner-stabilized, premixed, laminar flames [27], counterflow, laminar, diffusion flames [35], and the extinction problems we consider here.

The procedure we follow is similar to that used in the solution of one-dimensional, adiabatic, premixed, laminar flames [34]. For each value of the parameter s, we want to obtain the corresponding value of the strain rate and the remaining dependent solution components. We point out that for each value of the pseudo-arclength the strain rate is constant. Hence, it satisfies the trivial differential equation

$$\frac{d}{dy}\left(\frac{1}{a}\right) = 0. \tag{5.10}$$

We can maintain the block tridiagonal structure of the Jacobian in (5.7) if we introduce the reciprocal of the strain rate as a dependent variable at m of the $m+1$ grid points and if we specify a normalization condition at the remaining grid point that does not introduce nonzero Jacobian entries outside of the three block diagonals. The success of this procedure depends upon the choice of the normalization condition.

In premixed flame extinction studies (see, e.g., [3, 7]) the maximum temperature is used often as the ordinate in bifurcation curves. The maximum temperature is both a measurable quantity and one of practical interest. In the counterflowing premixed flames we consider here, the maximum temperature is attained at the symmetry plane $y=0$. Hence, it is natural to introduce the temperature at the first grid point along with the reciprocal of the strain rate as the dependent variables in the normalization condition. We do not include the remaining dependent variables. In this way the block tridiagonal structure of the Jacobian can be maintained.

The final form of the governing equations we solve is given by

$$\frac{dV}{dy}+a\rho f'=0, \tag{5.11}$$

$$\frac{d}{dy}\left(\frac{\lambda}{c_p}\frac{df'}{dy}\right)-V\frac{df'}{dy}+a(\rho_e-\rho(f')^2)=0, \tag{5.12}$$

$$\frac{d}{dy}\left(\frac{\lambda}{c_p}\frac{dT}{dy}\right)-V\frac{dT}{dy}+\frac{q}{c_p}=0, \tag{5.13}$$

$$\frac{d}{dy}\left(\frac{1}{a}\right)=0, \tag{5.14}$$

with the boundary conditions at $y=0$ given by

$$V=0, \tag{5.15}$$

$$\frac{df'}{dy}=0, \tag{5.16}$$

$$\frac{dT}{dy}=0, \tag{5.17}$$

$$\frac{dT(0,s_0)}{ds}(T(0,s)-T(0,s_0))+\frac{d}{ds}\left(\frac{1}{a}(0,s_0)\right)\left(\frac{1}{a}(0,s)-\frac{1}{a}(0,s_0)\right)-(s-s_0)=0, \tag{5.18}$$

and as $y\to\infty$ by

$$f'=1, \tag{5.19}$$

$$T=T_e. \tag{5.20}$$

6. Numerical Results

In this section we apply the one-step kinetics model and the modified arclength continuation procedure to determine the extinction limits as a function of the strain rate for counterflowing premixed hydrogen–air and methane–air flames. In all cases

values for the specific heats, the heat releases, the thermal conductivities, the pre-exponential constants and the activation energies used in (5.11)–(5.20) are taken from Coffee *et al.* [26]. For problems in which intermediate values are required, we apply a piecewise linear interpolation procedure to obtain the appropriate parameter values.

It is worthwhile to point out that several other procedures for calculating extinction points of premixed laminar flames in a stagnation point flow have appeared recently in the literature [6, 7, 10]. In the work of Sato and Tsuji [6, 7] an energy and a species conservation equation were solved with a Runge–Kutta shooting procedure. For a specified value of the temperature at the wall, response curves were obtained for the flame temperature versus the first Damköhler number (D_I). The computational procedure involved adjusting D_I and the mass fraction of the reactant on the wall so that the downstream boundary conditions were satisfied. In their study the Lewis number could be varied. In the work by Smith *et al.* [10] the full set of conservation equations with unit Lewis numbers were solved by a combination of shooting and quasilinearization. Extinction points and multiple solutions were found when a thin flame model and trial-and-error solution approximations were used as initial solution estimates. Our approach differs from that of Sato and Tsuji [6, 7] in that, like Smith *et al.* [10], we solve the coupled mass, momentum, species, and energy conservation equations. We employ an adaptive finite difference method. However, unlike the procedure used by Smith *et al.*, we are able to trace out automatically all of the physical and unphysical solutions with the pseudo-arclength continuation procedure starting from a single solution.

Methane–Air Flames

We performed a sequence of calculations for both lean and rich methane–air flames. For each methane–air mixture the modified arclength continuation procedure was implemented to obtain profiles of the maximum temperature versus the inverse of the strain rate. The adaptive boundary value solution method (see Sect. 4) was used first to obtain a solution for a methane–air mixture consisting of 6.5% methane (mole fraction) with an initial strain rate of $a = 500\text{s}^{-1}$. The Euler continuation procedure discussed in (5.8)–(5.9) was used then to help obtain solutions (both physical and unphysical) as the parameter s (and hence the strain rate) changed. The computations were performed on a domain of one cm.

For each strain rate calculation 60–80 adaptively chosen grid points were used. However, as the strain rate adjusted, the location of the flame front shifted as well. To prevent the adaptive gridding procedure from using all of the grid points of a previous strain rate calculation, we implemented a "skeleton" grid procedure similar to the one used in [36] to restrict the growth in the number of mesh points. Typically, one half of the mesh points from a previous stain rate calculation was used initially in each new strain rate calculation.

Once the 6.5% calculation was completed, we repeated the procedure for methane–air mixtures containing 6.85, 7.5, 8.5, 9.5 (stoichiometric), 10.5, 11.5, 12.5,

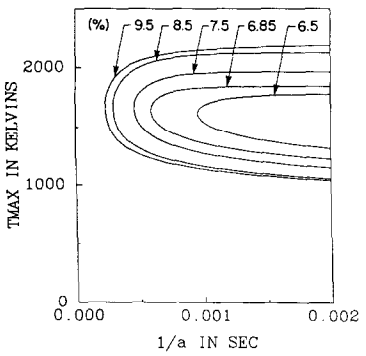

FIG. 3. C-shaped extinction curves for lean (6.5, 6.85, 7.5, 8.5%) and stoichiometric (9.5%) methane–air flames.

12.85, and 13.5% methane (mole fraction). In each case we obtained C-shaped extinction curves. The corresponding curves are plotted in Figs. 3 and 4. As the figures illustrate, as we move along the upper branch in the direction of increasing strain rate, the peak temperature decreases. Ultimately, as the value of $dT_{\max}/d(1/a) \to \infty$, the flame extinguishes. We can, however, continue past the extinction point with the arclength procedure. We find that, as the strain rate begins to decrease, the peak temperature continues to fall. Temperature profiles (both physical and unphysical) for an 11.5% methane (mole fraction) flame are illustrated in Figs. 5 and 6. If we decrease the strain rate even further, we will continue to move along the unphysical branch towards another turning point—an ignition point. After the ignition point is passed, we will move on to the extinguished solution branch. We have not included the ignition points since, from a practical point of view, they occur at strain rates so low that stabilization of such flames in the laboratory is exceedingly difficult (see also Smith *et al.* [10]).

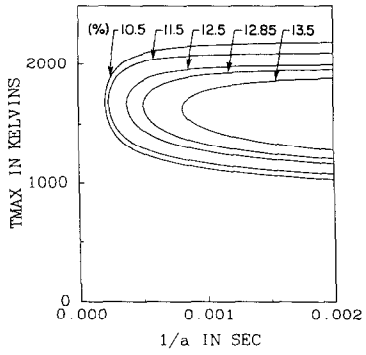

FIG. 4. C-shaped extinction curves for rich (10.5, 11.5, 12.5, 12.85, 13.5%) methane–air flames.

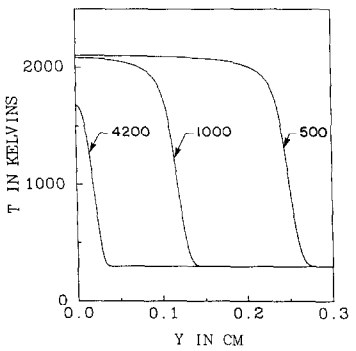

FIG. 5. Temperature profiles (physical) for an 11.5% methane–air flame. Profiles for strain rates of 500, 1000, and 4200 s^{-1} are illustrated.

If we collect the results of the ten methane–air flame calculations, we can plot the value of the strain rate and the velocity at extinction (at $x = 1$ cm.) versus the equivalence ratio. These results (the lack of smoothness in the curves is due to the number of calculations plotted) are contained in Figs. 7 and 8, respectively. We observe that the peak values of the strain rate and the corresponding extinction velocity occurred for slightly rich conditions—the flame with the highest calculated temperature. In addition, if we define the extinction distance as the distance from the plane of symmetry to the point at which the temperature is equal to 50% of its maximum temperature, we can obtain a plot of extinction distance versus equivalence ratio similar to the plots in Figs. 7 and 8. These results are shown in Fig. 9. It is worthwhile to point out that the results shown in Fig. 9 differ qualitatively from those reported by Sato [3] for lean methane–air mixtures. This is due primarily to the fact that we have assumed the Lewis numbers are equal to one.

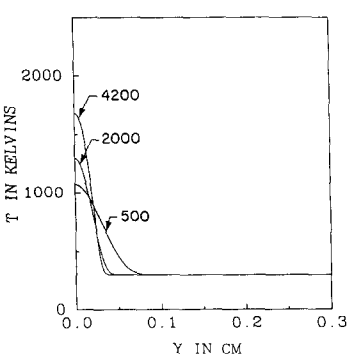

FIG. 6. Temperature profiles (unphysical) for an 11.5% methane–air flame. Profiles for strain rates of 500, 2000, and 4200 s^{-1} are illustrated.

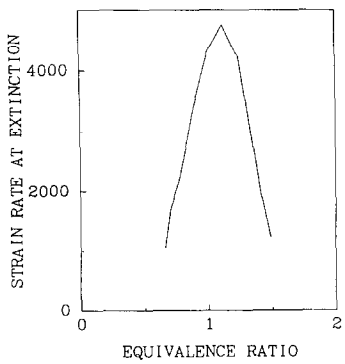

FIG. 7. Illustration of the strain rate (in s^{-1}) at extinction versus the methane–air equivalence ratio.

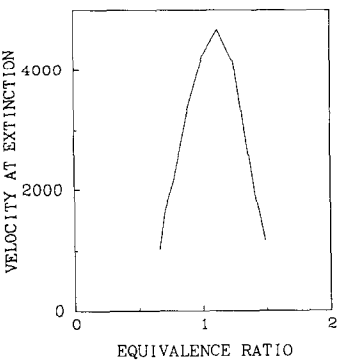

FIG. 8. Illustration of the velocity (in cm/s) at extinction versus the methane–air equivalence ratio.

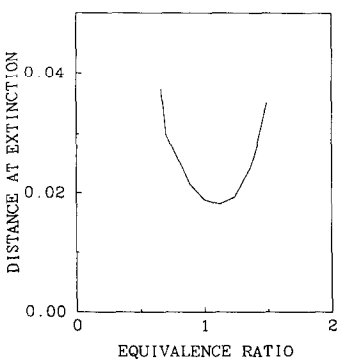

FIG. 9. Illustration of the distance (in cm) at extinction versus the methane–air equivalence ratio.

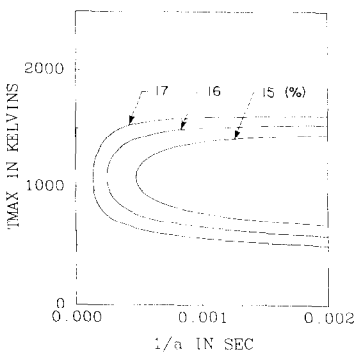

FIG. 10. *C*-shaped extinction curves for lean (15.0, 16.0, 17.0%) hydrogen–air flames.

Hydrogen–Air Flames

In the second test problem we considered, the solution procedure discussed in Sections 4 and 5 was applied to a set of premixed hydrogen–air flames. As in the methane–air calculations, we began the calculation with the strain rate equal to $500\,s^{-1}$. Again the Euler continuation procedure was used to help obtain solutions as s changed. The calculations were begun with a hydrogen–air mixture consisting of 15.0% hydrogen (mole fraction) on a computational domain of one cm. For each strain rate calculation we again used between 60–80 adaptively chosen grid points and the skeleton gridding procedure discussed in [36] was also used to restrict the growth of the unwanted grid points. In Fig. 10 we illustrate *C*-shaped extinction curves for flames consisting of 15, 16, and 17% hydrogen (mole fraction). The results are qualitatively similar to the curves illustrated in Figs. 3 and 4.

7. CONCLUSION

We have applied an arclength continuation procedure to calculate extinction limits for a set of premixed hydrogen–air and methane–air flames in a stagnation point flow. Profiles for the peak temperature versus the strain rate were obtained for a variety of incoming fuel–air mixtures. To simplify the computations, we considered a one-step global kinetics model in which all the Lewis numbers were assumed equal to one. We realize of course that such a procedure cannot predict adequately all of the detailed behavior resulting from a complex kinetics calculation. We have, however, illustrated the applicability of the numerical bifurcation procedure in calculating extinction limits for premixed flames in a stagnation point flow. In a subsequent paper we will apply the methods discussed in this study to obtain extinction limits of hydrogen–air and methane–air flames in which the chemistry is governed by a detailed multistep mechanism.

REFERENCES

1. S. ISHIZUKA AND C. K. LAW, *Nineteenth Symposium (International) on Combustion* (Reinhold, New York, 1982), p. 327.
2. C. K. LAW, S, ISHIZUKA, AND M. MIZOMOTO, *Eighteenth Symposium (International) on Combustion* (Reinhold, New York, 1982), p. 1791.
3. J. SATO, *Nineteenth Symposium (International) on Combustion* (Reinhold, New York, 1982), p. 1541.
4. G. I. SIVASHINSKY, *ACTA Astronaut.* **3**, 889 (1976).
5. J. BUCKMASTER, *Seventeenth Symposium (International) on Combustion* (Reinhold, New York, 1982), p. 835.
6. J. SATO AND H. TSUJI, *Sixteenth Symposium on Combustion, Japan*, 1978, p. 13.
7. J. SATO AND H. TSUJI, *Comb. Sci. Technol.* **33**, 193 (1983).
8. H. TSUJI AND I. YAMAOKA, *Nineteenth Symposium (International) on Combustion* (Reinhold, New York, 1982), p. 1533.
9. P. A. LIBBY AND F. A. WILLIAMS, *Comb. Sci. Technol.* **37**, 221 (1984).
10. H. W. SMITH, R. A. SCHMITZ, AND R. G. LADD, *Comb. Sci. Technol.* **4**, 131 (1971).
11. N. DARABIHA, S. CANDEL, AND F. E. MARBLE, in *Symposium on Numerical Simulation of Combustion Phenomena, INRIA* (Springer-Verlag, New York, 1985).
12. V. GIOVANGIGLI AND S. CANDEL, *Comb. Sci. Technol.* **48**, 1 (1986).
13. M. FANG, R. A. SCHMITZ, AND R. G. LADD, *Comb. Sci. Technol.* **4**, 143 (1971).
14. H. B. KELLER, in Applications of Bifurcation Theory, P. Rabinowitz, Ed., (Academic Press, New York, 1977).
15. A. JEPSON AND A. SPENCE, in *Numerical Methods for Bifurcation Problems*, T. Kupper, H. Mittelmann, and H. Weber, Eds., (Birkhauser, Basel, 1984).
16. T. CHAN, in *Numerical Methods for Bifurcation Problems*, T. Kupper, H. Mittelmann, and H. Weber, Eds., (Birkhauser, Basel, 1984).
17. R. SEYDEL, *Numer. Math.* **3**, 339 (1979).
18. R. F. HEINEMANN, K. A. OVERHOLSER, AND G. W. REDDIEN, *Chem. Eng. Sci.* **34**, 833 (1979).
19. R. F. HEINEMANN, K. A. OVERHOLSER, AND G. W. REDDIEN, *AIChE J.* **26**, 725 (1980).
20. G. DIXON-LEWIS, T. DAVID, P. H. HASKELL, S. FUKUTANI, H. JINNO, J. A. MILLER, R. J. KEE, M. D. SMOOKE, N. PETERS, E. EFFELSBERG, J. WARNATZ, AND F. BEHRENDT, *Twentieth Symposium (International) on Combustion*, (Reinhold, New York, 1982), p. 1893.
21. J. A. MILLER, R. E. MITCHELL, M. D. SMOOKE, AND R. J. KEE, *Nineteenth Symposium (International) on Combustion*, (Reinhold, New York, 1982), p. 181.
22. J. A. MILLER, M. D. SMOOKE, R. M. GREEN, AND R. J. KEE, *Comb. Sci. Technol.* **34**, 149 (1983).
23. A. LEVY AND F. J. WEINBERG, *Seventh Symposium (International) on Combustion*, (Reinhold, New York, 1959), p. 296.
24. A. LEVY AND F. J. WEINBERG, *Combust. Flame* **3**, 229 (1959).
25. C. K. WESTBROOK AND F. L. DRYER, *Comb. Sci. Technol.* **27**, 31 (1981).
26. T. P. COFFEE, A. J. KOTLAR, AND M. S. MILLER, *Combust. Flame* **54**, 155 (1983).
27. M. D. SMOOKE, *J. Comput. Phys.* **48**, 72 (1982).
28. P. DEUFLHARD, *Numer. Math.* **22**, 289 (1974).
29. M. D. SMOOKE, *J. Opt. Theory Appl.* **39**, 489 (1983).
30. J. KAUTSKY AND N. K. NICHOLS, *SIAM J. Sci. Stat. Comput.* **1**, 499 (1980).
31. R. D. RUSSELL, in *Proceedings, Conference for Working Codes for Boundary Value Problems in ODE's*, B. Childs *et al.*, Eds., (Springer-Verlag, New York, 1979).
32. V. PEREYRA AND E. G. SEWELL, *Numer. Math.* **23**, 261 (1975).
33. A. B. WHITE, *SIAM J. Numer. Anal.* **16**, 472 (1979).
34. M. D. SMOOKE, J. A. MILLER, AND R. J. KEE, *Comb. Sci. Technol.* **34**, 79 (1983).
35. M. D. SMOOKE, J. A. MILLER, AND R. J. KEE, in *Numerical Boundary Value ODEs*, U. M. Ascher and R. D. Russell, Eds., (Birkhauser, Basel, 1985).
36. M. D. SMOOKE AND M. L. KOSZYKOWSKI, *SIAM J. Sci. Stat. Comp.* **7**, 301 (1986).